JLB

Dexamethasone potentiates myeloid-derived suppressor cell function in prolonging allograft survival through nitric oxide

Jiongbo Liao,[*,†,1] *Xiao Wang,*[†,1] *Yujing Bi,*[‡,1] *Bo Shen,*[§,1] *Kun Shao,*[*,†,1] *Hui Yang,*[†] *Yun Lu,*[†]
Zhengguo Zhang,[†] *Xi Chen,*[†] *Huanrong Liu,*[†] *Jian Wang,*[†] *Yiwei Chu,*[†] *Lixiang Xue,*[‖,2]
Xianghui Wang,[*,2] *and Guangwei Liu*[†,2]

*Ruijin Hospital and Medical School of Shanghai Jiao Tong University, Shanghai, China; [†]Key Laboratory of Medical Molecular Virology of Ministries of Education and Health, Department of Immunology, School of Basic Medical Sciences, and Biotherapy Research Center, Institute of Immunobiology, and [§]Institute of Radiation Medicine, Fudan University, Shanghai, China; [‡]State Key Laboratory of Pathogen and Biosecurity, Beijing Institute of Microbiology and Epidemiology, Beijing, China; and [‖]Department of Biochemistry and Molecular Biology, Peking University, Health Science Center, Beijing, China

ABSTRACT

Whereas GCs have been demonstrated to be beneficial for transplantation patients, the pharmacological mechanisms remain unknown. Herein, the role of GR signaling was investigated via a pharmacological approach in a murine allogeneic skin transplantation model. The GC Dex, a representative GC, significantly relieved allograft rejection. In Dex-treated allograft recipient mice, CD11b$^+$Gr1$^+$ MDSCs prolonged graft survival and acted as functional suppressive immune modulators that resulted in fewer IFN-γ-producing Th1 cells and a greater number of IL-4-producing Th2 cells. In agreement, Dex-treated MDSCs promoted reciprocal differentiation between Th1 and Th2 in vivo. Importantly, the GR is required in the Dex-induced MDSC effects. The blocking of GR with RU486 significantly diminished the expression of CXCR2 and the recruitment of CD11b$^+$Gr1$^+$ MDSCs, thereby recovering the increased MDSC-suppressive activity induced by Dex. Mechanistically, Dex treatment induced MDSC iNOS expression and NO production. Pharmacologic inhibition of iNOS completely eliminated the MDSC-suppressive function and the effects on T cell differentiation. This study shows MDSCs to be an essential component in the prolongation of allograft survival following Dex or RU486 treatment, validating the GC–GR–NO signaling axis as a potential therapeutic target in transplantation.
J. Leukoc. Biol. 96: 675–684; 2014.

Introduction

Synthetic GC immunosuppressants, especially Dex, have been widely used in treating inflammatory disorders and are well-known for their effect on the immune system [1, 2]. It has been suggested that GCs regulate a variety of different immune cell activities. Dex can alter the phenotype and function of DCs, rendering them tolerogeneic [3]. Moreover, Dex has been regarded as a tolerogeneic adjuvant through the in vivo selection of tolerogeneic macrophages [4]. Furthermore, Dex combined with peptide antigens was shown to induce the expansion of antigen-specific CD4$^+$Foxp3$^+$ T_{regs} that persist in vivo and are used in the prevention of autoimmune diabetes [5]. In transplantation, GC has also been demonstrated to be beneficial for patients in clinical applications [6, 7]. However, the immunological mechanisms of GC in transplantation remain to be elucidated.

MDSCs comprise a heterogeneous cell population that suppresses T cell proliferation and function, blocks NK cell cytotoxicity, and promotes the development of T_{regs} in tumor-bearing hosts [8–10]. MDSCs have been detected in the blood of cancer patients, as well as the BM, spleen, and peripheral blood of tumor-bearing mice [11, 12]. In transplantation, MDSCs contribute to kidney and cardiovascular graft tolerance [13, 14]. A recent study showed that prednisone induces increased MDSC recruitment and CD4$^+$Foxp3$^+$ T_{reg} expansion in human kidney transplant recipients [15]. However, the

1. These authors contributed equally to this work as cofirst authors.
2. Correspondence: Fudan University, Yixueyuan Rd. 138, Xuhui District, Shanghai, China, 200032, E-mail: liugw@fudan.edu.cn (G.L.); Shanghai Jiao Tong University, Ruijin Er Rd. 197, Huangpu District, Shanghai, China, 200025, E-mail: wxh@medmail.com.cn (X.W.); Peking University, Xueruan Rd. 38, Haidian District, Beijing, China, 100191, E-mail: lixiangxue@bjmu.edu.cn (L.X.)

MDSC regulatory mechanisms of GCs in transplantation remain unclear.

In the present study, we sought to determine whether MDSCs comprise an essential immune component in GC-prolonged allograft survival. Dex treatment significantly ameliorated graft rejection and pathological injury. In addition, it significantly reduced inflammatory cell infiltration concomitantly with enhanced CD11b$^+$Gr1$^+$ MDSC accumulation in the allograft. These cells are required for the Dex-prolonged allograft survival. Mechanistically, targeting the GR, Dex treatment potentiated MDSC recruitment and function and consequentially, promoted a reciprocal differentiation of Th1 and Th2 in the murine allograft. Thus, the current study shows MDSCs to be an essential immune component in GC–GR amelioration of allograft rejection.

MATERIALS AND METHODS

Mice

All animal experiments were performed in accordance with the approval of the Animal Ethics Committee of Fudan University (Shanghai, China). CD45.1$^+$ B6 and OTII mice were obtained from the Center of Model Animal Research at Nanjing University (China). BALB/c and B6 (CD45.2$^+$) mice were obtained from the Fudan University Experimental Animal Center. All mice were bred and maintained in specific pathogen-free conditions. Sex-matched littermates at 6–8 weeks of age were used in the experiments described in this study.

Skin transplantation, Dex treatment, and histological analysis

Skin from BALB/c mice was transplanted into B6 recipients as described previously [16–19]. Recipient mice were injected i.p. with Dex (5 mg/kg body weight) daily, starting on Day 1 (6 h before the transplantation with allogeneic skin). For skin transplantation, erythema, edema, and hair loss were considered early signs of rejection, whereas ulceration, progressive shrinkage, and desquamation were considered to be the endpoints of rejection [20]. Photographs were taken daily with a digital camera (Canon PowerShot A640; Tokyo, Japan), until the graft was rejected completely. The skin grafts were removed as the indicated time-points and rinsed in cold PBS, placed in optimal cutting temperature compound, and frozen immediately in liquid nitrogen for histopathological examination. Sections (4–6 μm) were fixed in 4% paraformaldehyde and stained with H&E for the assessment of cellular infiltration.

mAb and flow cytometry

For the FCM analysis of cell-surface markers, cells were stained with antibodies in PBS containing 0.1% (wt/vol) BSA and 0.1% NaN$_3$. The following antibodies were obtained from eBioscience (San Diego, CA, USA): anti-CD11b (M1/70), anti-F4/80 (BM8), anti-Gr-1 (RB6-8C5), anti-CD4 (GK1.5), anti-CD11c (N418), anti-NK1.1 (Ly-55), anti-CD44 (IM7), anti-CD62L (MEL-4), anti-CD80 (16-10A1), anti-CD86 (GL1), anti-CD40 (1C10), anti-CD54 (YN1/1.7.4), and anti-CXCR4 (2B11). The following antibodies were obtained from BD Biosciences (San Jose, CA, USA): anti-CD45 (TU116), anti-CD8 (53-6.7), anti-CD115 (AFS98), and anti-CXCR2 (242216). Anti-CD3 (145-2C11) and -CD19 (6D5) were obtained from Miltenyi Biotec (Bergisch Gladbach, Germany). Anti-Ly6G (RB6-8C5) and anti-GR (ab984) were obtained from Abcam (Cambridge, UK).

Intracellular staining was analyzed by FCM, according to the manufacturer's instructions, with modifications as described [21]. For cytokine expression analysis, cells isolated from the indicated organs were restimulated with LPS (L2630; Sigma-Aldrich, St. Louis, MO, USA) for 5 h for CD11b$^+$Gr1$^+$ cell analysis or restimulated with PMA (P-8139; Sigma-Aldrich) and ionomy-

cin (I-0634; Sigma-Aldrich) for 5 h for CD4$^+$ T cell or CD8$^+$ T cell analysis, and GolgiStop (554724; BD Biosciences) was added for the last 2 h. After surface staining and washing, the cells were fixed immediately with Cytofix/Cytoperm solution (554714; BD Biosciences) and were stained with anti-TNF-α (MP6-XT22), anti-IL-10 (JES5-16E3), anti-IL-4 (11B11), and anti-IFN-γ (XMG1.2) from eBioscience. For Foxp3 expression analysis, after surface staining, cells were fixed with Fixation/Permeabilization buffer (00–5523; eBioscience) and stained with anti-Foxp3 (FJK-16s; eBioscience). The FCM data were acquired on a FACSCalibur (Becton Dickinson, San Diego, CA, USA) or an Epics XL bench-top flow cytometer (Beckman Coulter, Brea, CA, USA), and data were analyzed with FlowJo (TreeStar, San Carlos, CA, USA). The cell numbers of the various populations were calculated by multiplying the percentage of cells of interest by the total cell number.

Cell isolation and purification

For the isolation of skin-graft cells, skin grafts were retrieved and minced into small pieces with a scalpel and then digested for ~1 h at 37°C in RPMI-1640 medium containing 30 U/mL collagenase (type IV; Sigma-Aldrich) and 1 mM CaCl$_2$. Collagenase-pretreated tissues were then ground with the plunger of a 5-mL disposable syringe and passed through a 70-μm nylon cell strainer. Cells were collected by centrifugation at 300 g for 15 min and resuspended in FACS staining buffer for cell-marker staining.

Following cardiac perfusion with PBS, the spleen was aseptically removed and mechanically disrupted between sterile-frosted microscope slides, as described previously [22, 23]. Splenic CD11b$^+$ cells were isolated using anti-CD11b magnetic beads and positive-selection columns (Miltenyi Biotec). Gr1$^+$ cells were isolated using anti-Gr1-PE mAb (RB6-8C5; eBioscience) and positive immunomagnetic separation with a selection kit (Stem Cell Technologies, Vancouver, BC, Canada) or sorted on a FACSAria II (Becton Dickinson). Lymphocytes were isolated from the lymph nodes, and naive T cells (CD4$^+$CD62L^{hi} CD44^{lo}CD25$^-$) were sorted on a FACSAria II, as described [24]. Flow cytometry verified that all of the isolated cells yielded a >90% pure population.

Quantitative RT-PCR

Total RNA from the skin grafts or spleen of the allograft recipients was isolated using RNeasy columns, and contaminating DNA was removed by on-column treatment with RNase-free DNase (Qiagen, Dusseldorf, Germany). RNA was extracted with an RNeasy kit (Qiagen), and cDNA was synthesized using SuperScript III RT (Invitrogen, Carlsbad, CA, USA). An ABI 7900 real-time PCR system was used for quantitative PCR, with the primers and probe sets obtained from Applied Biosystems (Carlsbad, CA, USA; see **Table 1**). Results were analyzed using SDS 2.1 software (Applied Biosystems). The C_T value of the endogenous control gene (*Hprt1*, encoding HPRT) was subtracted from the ΔC_T. The expression of each target gene is presented as the "fold change" relative to that of the control samples ($2^{-\Delta\Delta CT}$), as described previously [24].

In vivo and in vitro functional assay of CD11b$^+$Gr1$^+$ cells

For depleting CD11b$^+$Gr1$^+$ cells in vivo, 0.5 mg depleting anti-Gr-1 mAb (RB6-8C5) was i.p.-administered to recipients on Day −1 before skin transplantation. For detection of the immunosuppression of CD11b$^+$Gr1$^+$ cells in vivo, WT mice were transplanted with BALB/c skin grafts. Seven days later, CD11b$^+$Gr1$^+$ cells (1×10^6) from the spleens of PBS and Dex-treated allograft recipient mice were sorted and i.v.-injected into syngeneic B6 mice. One day after adoptive transfer, these mice were grafted with BALB/c skin, and the skin graft was followed daily.

For the suppression assay in vitro, CD11b$^+$Gr1$^+$ cells sorted from the spleen of PBS or Dex-treated allograft B6 recipients, 7 days after alloskin transplantation, were added to a MLR system. The suppressive function of MDSCs was assessed by determining their ability to inhibit T cell activation, as described previously [25]. B6 CD4$^+$ T cells (1×10^5 cells/well) were cocultured with 15 μg/mL mitomycin C-pretreated BALB/c splenocytes (1×10^5 cells/well), and CD11b$^+$Gr1$^+$ cells (1×10^5 cells/well) were sorted

TABLE 1. Primer Sequences Used for Real-Time PCR Assays

Genes	Forward primer	Reverse primer
Arg1	5′-CCAGAAGAATGGAAGAGTCAGTGT-3′	5′-GCAGATATGCAGGGAGTCACC-3′
Foxp3	5′-GGCCCTTCTCCAGGACAGA-3′	5′-GGCATGGGCATCCACAGT-3′
iNOS	5′-CACCAAGCTGAACTTGAGCG-3′	5′-CGTGGCTTTGGGCTCCTC-3′
IFN-γ	5′-GAACTGGCAAAAGGATGGTGA-3′	5′-TGTGGGTTGTTGACCTCAAAC-3′
IL-4	5′-TTGTCATCCTGCTCTTCTTTCTC-3′	5′-CAGGAAGTCTTTCAGTGATGTGG-3′
RORγt	5′-CCGCTGAGAGGGCTTCAC-3′	5′-TGCAGGAGTAGGCCACATTACA-3′
T-bet	5′-AGCAAGGACGGCGAATGTT-3′	5′-GGGTGGACATATAAGCGGTTC-3′
TNF-α	5′-CTGAACTTCGGGGTGATCGG-3′	5′-GGCTTGTCACTCGAATTTTGAGA-3′
HPRT	5′-CCTAAGATGAGCGCAAGTTGAA-3′	5′-CCACAGGACTAGAACACCTGCTAA-3′
GATA3	5′-GAATCCTCTGCATCAACAAGC-3′	5′-GGGCAAGGGTTCTGAGGT-3′
GR	5′-ACTGCCCCAAGTGAAAACAGA-3′	5′-GCCCAGTTTCTCCTGCTTAATTAC-3′

at different ratios in a flat-bottom, 96-well plate at 37°C in 5% CO_2. Cell proliferation was determined 72 h after incubation with ^{3}H-thymidine for the last 16 h of culture. L-NMMA (5 mM; Sigma-Aldrich) was added at the beginning of the culture to block the NO pathway.

DTH

Approximately 2 weeks after the OTII mice were immunized with OVA antigen (1 mg/ml), OTII CD4$^+$ T cells of the spleen and lymph nodes were enriched using the negative-selection MACS kit for CD4$^+$ T lymphocytes (Miltenyi Biotec). CD11b$^+$Gr1$^+$ cells (5×10^5 cells each) isolated from the spleen B6 mice or PBS or Dex-treated allograft recipient mice were used as APCs for OVA. Responder cells (OTII CD4$^+$ T cells) and CD11b$^+$Gr1$^+$ cells (5×10^5 cells each), with or without OVA, were injected i.d. into the pinnate of naive CD45.1$^+$ B6 mice. The changes in ear thickness were measured using an Engineer's micrometer, 48 h after challenge. The ear-thickness changes were calculated by subtracting the thickness of the same ear before injection from that of the thickness after injection, as described previously [26].

Cell proliferation and apoptosis assay

To detect the proliferation of CD11b$^+$Gr1$^+$ cells in vivo, 150 μl of a 10-mg/mL BrdU solution was injected into mice, as described previously [27]. Recipient splenic cells were isolated and BrdU$^+$ cells visualized using the BrdU flow kit (BD Biosciences). Samples were also stained with CD11b and Gr1 to visualize MDSCs. Apoptosis of MDSCs in recipient mouse splenic cells was assayed by flow cytometry using Annexin V staining (BD PharMingen, San Diego, CA, USA) with a gating strategy aligned to analyze CD11b$^+$-Gr1$^+$ cells, as described previously [28]. Flow cytometry data were acquired on a FACSCalibur and analyzed using FlowJo software.

NO production assay

After incubating equal volumes of culture supernatant or serum (100 μl) with Greiss reagent (G4410; Sigma-Aldrich), the absorbance at 550 nm was measured at a wavelength of 550 nm using a microplate reader (Bio-Rad, Hercules, CA, USA), as described previously [25].

Statistical analyses

All data are presented as the mean ± SD. Student's unpaired *t*-test for comparison of means was used to compare differences between groups. Comparison of the survival curves was performed using the log-rank (Mantel-Cox) test. $P < 0.05$ (α-value) was considered to be statistically significant.

RESULTS

Dex prolongs allograft survival

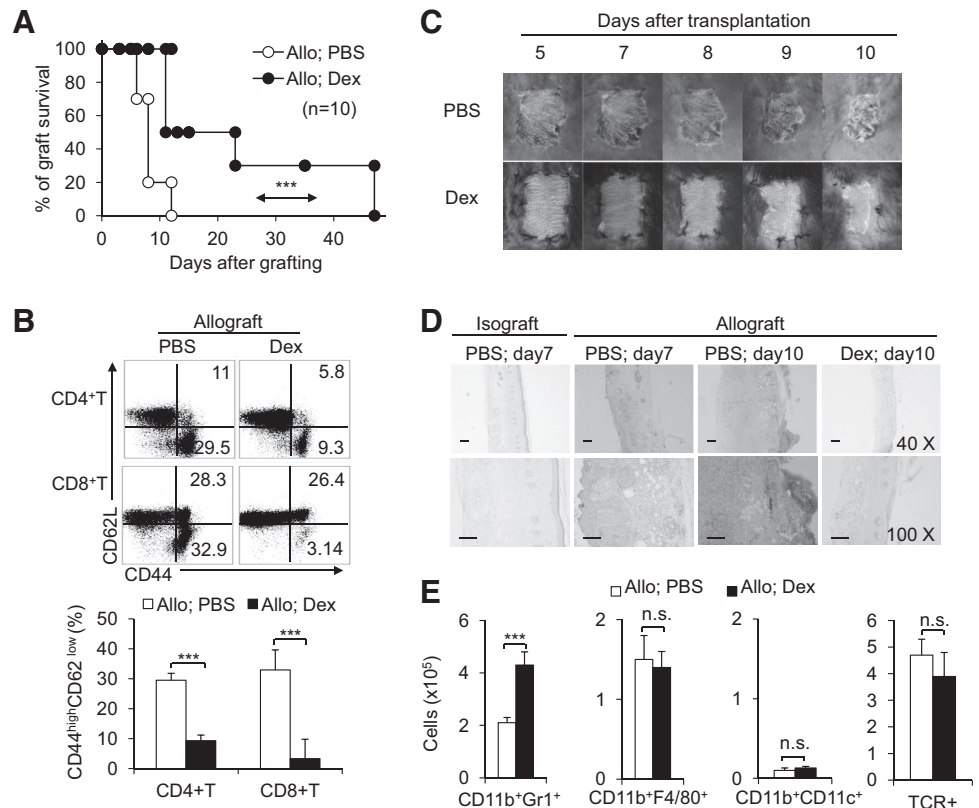We first investigated the effects of Dex on allograft survival. As shown in **Fig. 1A**, the daily treatment with Dex (5 mg/kg body weight) or PBS (solvent) was started 6 h before transplantation with allogeneic BALB/c skin. Dex treatment significantly prolonged allograft survival compared with the control PBS treatment group. Moreover, the allograft recipient mouse T cells displayed a lower autoimmune phenotype in Dex-treated recipient mice than control mice (Fig. 1B). Consistent with this finding, from Day 5 to 10, the alloskin grafts on the PBS control recipients exhibited a progressive loss of hair, dermal necrosis, and scab formation, as shown in Fig. 1C. However, the graft on the Dex-treated recipients had a normal gross appearance and hair growth. Histological examination of the skin allograft revealed mild immune-cell infiltrates in the derma of the skin grafts in the Dex-treated recipients on Days 7 and 10 after grafting compared with the PBS control recipients, which displayed moderate infiltrates and necrosis (Fig. 1D). We next analyzed the graft inflammatory cell infiltration in the allograft treated with PBS or Dex. Single-cell suspensions from the grafted skin of Dex-treated mice and control mice were isolated and analyzed by FCM. As showed in Fig. 1E, a significantly higher number of CD11b$^+$Gr1$^+$ cells, but not CD11b$^+$F4/80$^+$ macrophages, CD11b$^+$ CD11c$^+$ DCs, or T (CD4$^+$ T or CD8$^+$ T) cells, were found in the Dex-treated graft compared with the control group. These data collectively suggest that CD11b$^+$Gr1$^+$ cells are involved in Dex-prolonged allograft survival.

Dex treatment up-regulates the expression of chemokines that mediates CD11b$^+$Gr1$^+$ cell recruitment in prolonging allograft survival

To confirm the apparent CD11b$^+$Gr1$^+$ cell-number alteration, we analyzed the infiltrating cells in the allograft and recipient mouse dLNs, spleen, blood, and BM. Dex-treated allograft recipients consistently exhibited a higher CD11b$^+$-Gr1$^+$ cell percentage than the PBS-treated control (**Fig. 2A and B**). Moreover, in the inflamed dLNs, Dex-treated recipient mice exhibited more CD11b$^+$Gr1$^+$ cell infiltration than the control group (Fig. 2C). Collectively, these data indicate that systemic CD11b$^+$Gr1$^+$ cell infiltration from the BM into the local inflammatory site is critical for prolonging allograft survival.

The increased frequency of infiltrating CD11b$^+$Gr1$^+$ cells might have occurred from a decrease in cell death, an increase in differentiation from progenitors, or an enhanced

Figure 1. Dex treatment significantly relieved allograft rejection and promoted CD11b⁺Gr1⁺ cell infiltration in grafted skin. Age-matched WT B6 mice were injected i.p. with PBS (solvent) or Dex (5 mg/kg body weight) daily, starting at 6 h before transplantation with allogeneic BALB/c skin, respectively. (A) Dex treatment significantly relieved the alloskingraft (Allo) rejection compared with the control group. (B) The expression of CD44 and CD62L on the CD4⁺ T and CD8⁺ T cells was analyzed in the allograft recipient mice and a typical FCM figure. The data were summarized (lower). (C) Macroscopic pictures of alloskin grafts at different time-points. (D) The pathological changes in the skin allografts on Days 7 and 10. (E) Increased CD11b⁺Gr1⁺ cell infiltration, but not that of CD11b⁺F4/80⁺ macrophages, CD11b⁺CD11c⁺ DCs, and TCR⁺ T cells, was observed in alloskin grafts in the Dex-treated recipients. (B–E) Data are representative of three independent experiments ($n=3–5$). ***$P < 0.001$ compared with the indicated groups; n.s., not significant.

recruitment into the allograft. However, Dex treatment did not significantly change the cell death kinetics of graft CD11b⁺Gr1⁺ cells in the Dex-treated group (Supplemental Fig. 1A). Thus, it is unlikely that Dex altered the survival of CD11b⁺Gr1⁺cells. In addition, the percentage (Supplemental Fig. 1B) and the absolute cell number (data not shown) of BrdU⁺CD11b⁺Gr1⁺ cells were identical in the Dex-treated group and control group, suggesting no defects in cell proliferation following Dex treatment. However, the expression of CXCL1 and CXCL2, but not CCL3 or CCL5, chemokines that are known to regulate CD11b⁺Gr1⁺ cell migration [29–32] was up-regulated significantly following Dex treatment (Fig. 2D). In addition, the expression of CXCR2, the receptor for chemokines CXCL1 and CXCL2, was up-regulated in the CD11b⁺Gr1⁺ cells following Dex treatment (Fig. 2E). Furthermore, the induction of chemotactic factors in CD11b⁺Gr1⁺ MDSCs preceded the infiltration into the graft. Adoptively transferred, Dex-treated CD11b⁺Gr1⁺ MDSCs, which had been pretreated previously with an anti-CXCR2 antibody, did not alter the infiltration of donor cells into the allograft (Supplemental Fig. 1C) or show any effect on graft survival (Supplemental Fig. 1D). Finally, an anti-CXCR2 antibody injection blocked the CD11b⁺Gr1⁺ MDSC infiltration (Fig. 2F) and consequently, resulted in severe pathological damage and a rejection response (Fig. 2G). Altogether, these observations show that Dex promoted the recruitment of CD11b⁺Gr1⁺ MDSCs in the allograft recipient mice.

Myeloid CD11b⁺Gr1⁺cells are required for Dex prolongation of allograft survival

We examined whether CD11b⁺Gr1⁺ cells that accumulated following Dex treatment and have the characteristics of immune suppressors are reported for MDSCs [9, 10, 33]. Compared with cells isolated from the control group, CD11b⁺Gr1⁺ cells isolated from the Dex-treated allograft recipient spleen (**Fig. 3A**) and allograft (Fig. 3B) displayed significantly enhanced immunosuppression of T cell proliferation than controls in vitro. Additionally, splenic CD11b⁺Gr1⁺ cells following Dex treatment displayed a MDSC phenotype, CXCR4^high, CD115^high, CD44^high, CD86^low, and CD54^low, but with identical levels of CD62L and CD80 (Supplemental Fig. 2A). Moreover, Dex-treated CD11b⁺Gr1⁺ cells produced lower TNF-α and higher IL-10 levels in the allograft recipient mice compared with the control group (Fig. 3C) in a time-dependent manner (Fig. 3D). We depleted these cells further by injecting anti-Gr1 mAb, as described previously [25]. Efficient depletion of CD11b⁺Gr1⁺ cells was achieved in these mice, as evidenced by FCM (data not shown). Strikingly, the depletion of Gr1⁺ cells significantly reduced Dex-ameliorated allograft rejection, as indicated by the changes in graft survival (Fig. 3E). Importantly, adoptive transfer of sorted CD11b⁺Gr1⁺ cells from Dex-treated allograft recipient mice but not the control group, into WT B6 recipients, significantly prolonged the percentage of allograft survival (Fig. 3F). These findings suggest that CD11b⁺Gr1⁺ MDSCs are required for Dex-mediated, protective effects in prolonging allograft survival.
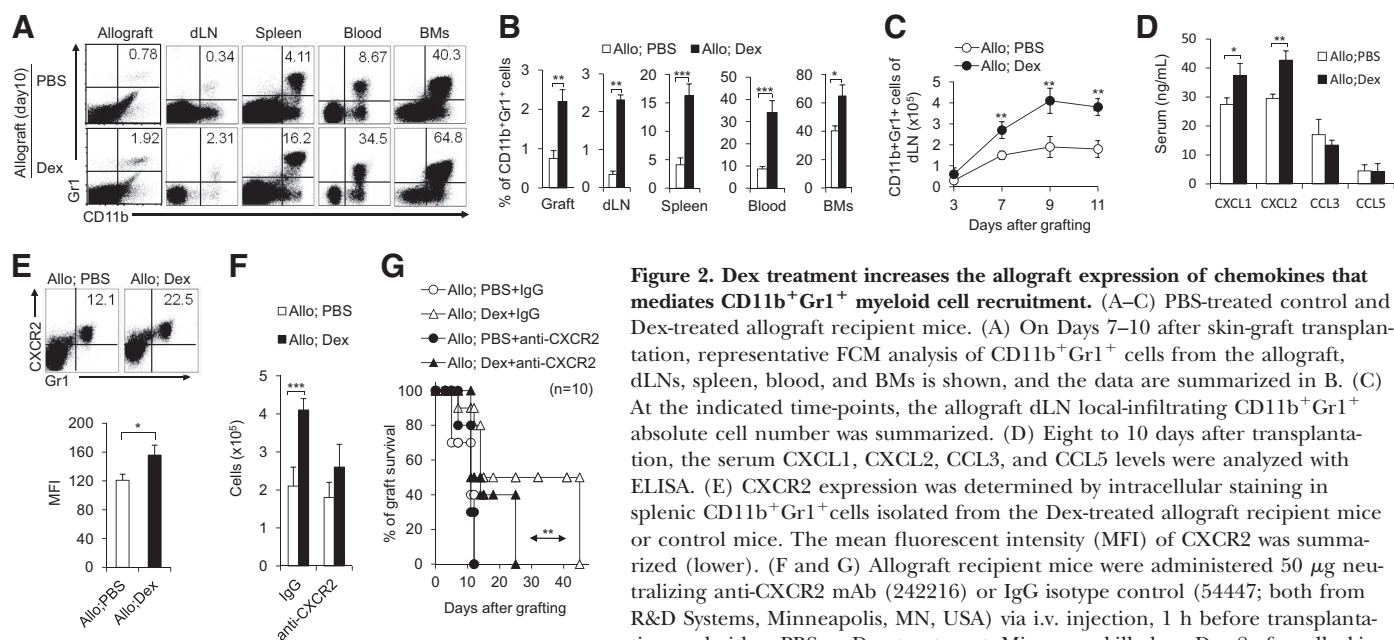
Figure 2. Dex treatment increases the allograft expression of chemokines that mediates CD11b⁺Gr1⁺ myeloid cell recruitment. (A–C) PBS-treated control and Dex-treated allograft recipient mice. (A) On Days 7–10 after skin-graft transplantation, representative FCM analysis of CD11b⁺Gr1⁺ cells from the allograft, dLNs, spleen, blood, and BMs is shown, and the data are summarized in B. (C) At the indicated time-points, the allograft dLN local-infiltrating CD11b⁺Gr1⁺ absolute cell number was summarized. (D) Eight to 10 days after transplantation, the serum CXCL1, CXCL2, CCL3, and CCL5 levels were analyzed with ELISA. (E) CXCR2 expression was determined by intracellular staining in splenic CD11b⁺Gr1⁺cells isolated from the Dex-treated allograft recipient mice or control mice. The mean fluorescent intensity (MFI) of CXCR2 was summarized (lower). (F and G) Allograft recipient mice were administered 50 μg neutralizing anti-CXCR2 mAb (242216) or IgG isotype control (54447; both from R&D Systems, Minneapolis, MN, USA) via i.v. injection, 1 h before transplantation and either PBS or Dex treatment. Mice were killed on Day 8 after alloskin transplantation, and the allograft local-infiltrating CD11b⁺Gr1⁺ cell number (F) was analyzed using FCM. (G) The graft survival data were plotted. Data are representative of four (A–C) or three (D and E) independent experiments (A–F; n=4–5). *$P < 0.05$; **$P < 0.01$; and ***$P < 0.001$ compared with the indicated groups.

GR is critical for Dex-induced CD11b⁺Gr1⁺ MDSC recruitment and function in prolonging allograft survival

To ascertain how Dex induces CD11b⁺Gr1⁺ MDSCs in allografts, we investigated GR expression, as it is regarded as essential to the GC effects. As shown in **Fig. 4A** and **B**, Dex treatment significantly up-regulated the expression of GR in allograft recipient mice at the protein and mRNA levels compared with the control group. This suggests that the GR is probably involved in the Dex-induced MDSC effects. The blocking of
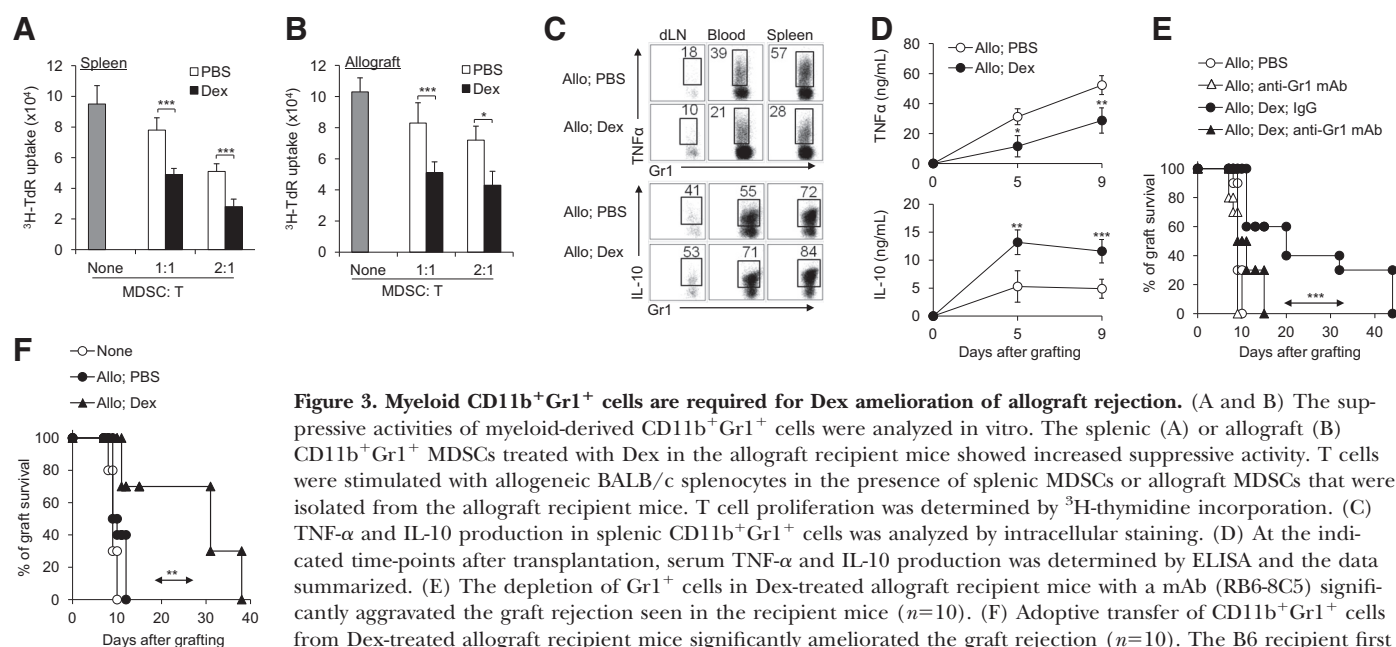

Figure 3. Myeloid CD11b⁺Gr1⁺ cells are required for Dex amelioration of allograft rejection. (A and B) The suppressive activities of myeloid-derived CD11b⁺Gr1⁺ cells were analyzed in vitro. The splenic (A) or allograft (B) CD11b⁺Gr1⁺ MDSCs treated with Dex in the allograft recipient mice showed increased suppressive activity. T cells were stimulated with allogeneic BALB/c splenocytes in the presence of splenic MDSCs or allograft MDSCs that were isolated from the allograft recipient mice. T cell proliferation was determined by ³H-thymidine incorporation. (C) TNF-α and IL-10 production in splenic CD11b⁺Gr1⁺ cells was analyzed by intracellular staining. (D) At the indicated time-points after transplantation, serum TNF-α and IL-10 production was determined by ELISA and the data summarized. (E) The depletion of Gr1⁺ cells in Dex-treated allograft recipient mice with a mAb (RB6-8C5) significantly aggravated the graft rejection seen in the recipient mice (n=10). (F) Adoptive transfer of CD11b⁺Gr1⁺ cells from Dex-treated allograft recipient mice significantly ameliorated the graft rejection (n=10). The B6 recipient first underwent transplantation, and on Days 7–8, a total of 1×10^6 CD11b⁺Gr1⁺ cells was sorted from the spleen of Dex- or PBS-treated control mice and transferred into the B6 recipient mice via i.v. injection. After 10–12 h, both groups underwent allograft skin transplantation, and the graft-survival curve was plotted (10 mice/group). Data are representative of three (A and B), four (C), or two (D) independent experiments (A–D; n=4–5). *$P < 0.05$; **$P < 0.01$; and ***$P < 0.001$ compared with the indicated groups.
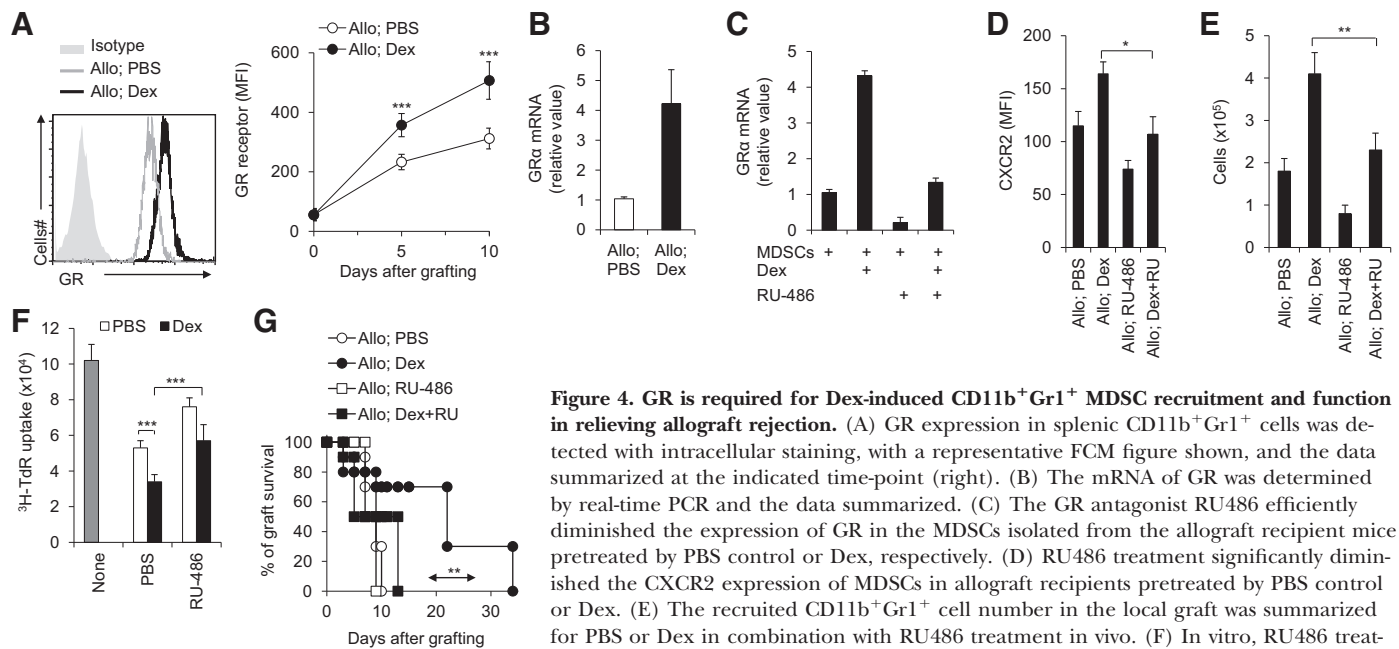
Figure 4. GR is required for Dex-induced CD11b+Gr1+ MDSC recruitment and function in relieving allograft rejection. (A) GR expression in splenic CD11b+Gr1+ cells was detected with intracellular staining, with a representative FCM figure shown, and the data summarized at the indicated time-point (right). (B) The mRNA of GR was determined by real-time PCR and the data summarized. (C) The GR antagonist RU486 efficiently diminished the expression of GR in the MDSCs isolated from the allograft recipient mice pretreated by PBS control or Dex, respectively. (D) RU486 treatment significantly diminished the CXCR2 expression of MDSCs in allograft recipients pretreated by PBS control or Dex. (E) The recruited CD11b+Gr1+ cell number in the local graft was summarized for PBS or Dex in combination with RU486 treatment in vivo. (F) In vitro, RU486 treatment ameliorated the suppression activity of MDSCs induced by Dex. (G) RU486 treatment significantly diminished graft survival in the Dex-treated allograft recipient mice. Data are representative of two (A–C), four (D), or three (F) independent experiments (A–F; n=3–5). *P < 0.05; **P < 0.01; and ***P < 0.001 compared with the indicated groups.

the GC signal with RU486 (a GR inhibitor) efficiently down-regulated GR expression in MDSCs in allograft recipient mice (Fig. 4C). Interestingly, RU486 treatment significantly diminished CXCR2 expression (Fig. 4D) and reduced the recruitment of CD11b+Gr1+ MDSCs in the allograft recipient mice (Fig. 4E). RU486 treatment also restored the suppressive activities of MDSCs in the Dex-treated allograft recipient mice (Fig. 4F), leading to the diminished graft survival seen in these animals (Fig. 4G). Taken together, these data suggest that GCs (Dex) promote MDSC recruitment and functional activities in allografts through a GR-dependent signaling pathway.

Dex modulates reciprocal Th1 and Th2 cell differentiation during allograft transplantation

Compared with control allograft recipient mice, Dex treatment resulted in a significantly ameliorated autoimmune phenotype (higher CD4+TCR+CD44highCD62low cells) in the dLNs and spleen of allograft recipient mice compared with the PBS-treated control group (**Fig. 5A**). Dex treatment also resulted in a significantly lower level of IFN-γ in the dLNs and spleen (Fig. 5B). In addition, a reciprocal decrease of IFN-γ-producing Th1 cells and an increase in IL-4-producing Th2 cells, but not "induced Foxp3+ T_regs", were observed in the dLNs and spleen of allograft recipients following Dex treatment (Fig. 5B). Similarly, the mRNA level of IFN-γ and IL-4 decreased and increased following Dex treatment in a time-dependent manner, respectively (Fig. 5C). Furthermore, specific T cell lineage transcriptional-factor expression provided evidence consistent with this finding (Fig. 5C). Finally, the depletion of Gr1+ cells in the Dex-treated but not the control group clearly restored the Th1 and Th2 cells in the dLNs of the allograft recipient mice (Supplemental Fig. 2B). Collectively, these data

suggest that MDSCs mediate reciprocal T cell differentiation of type Th1 and Th2, as a result, contributing to Dex-prolonged allograft survival.

Dex-induced MDSCs promote the reciprocal differentiation of T cells

The serum IFN-γ and IL-4 levels in the recipient mice were decreased and increased significantly in the Dex-treated allograft recipient mice, respectively, compared with control (**Fig. 6A**). Whereas the mRNA expression levels of Foxp3 and RORγt were comparable with the control, GATA3 mRNA and T-bet mRNA were increased and decreased, respectively, in Dex-treated allograft recipient mice (Fig. 6B). Furthermore, we investigated directly whether MDSCs regulate the reciprocal T cell differentiation in vivo and whether the regulation of T cell differentiation contributes to prolonged allograft skin survival. DTH experiments were used to investigate the suppressive activity of MDSCs in vivo, as described previously [26]. Approximately 2 weeks after OTII mice were immunized with OVA peptide, CD4+ T cells of spleens and lymph nodes were enriched. We then isolated the CD11b+Gr1+ cells from Dex-treated allograft recipient mice and PBS-treated control mice. Responder cells (CD4+ T cells) and CD11b+Gr1+ cells (5×10^5 cells each) in the presence of antigen were injected i.d. into the pinnate of naive B6 mice. The change in ear thickness was measured, and the Dex-treated MDSC cotransferred groups exhibited a diminished DTH (Fig. 6C). At 48 h after transfer, the donor CD4+ T cells of the dLNs were isolated and exhibited higher IL-4 and lower IFN-γ without any change in Foxp3 expression observed in the Dex-treated MDSC cotransfer groups (Fig. 6D). In agreement with this, the mRNA expression of IL-4 and IFN-γ, but not IL-17A, was in-
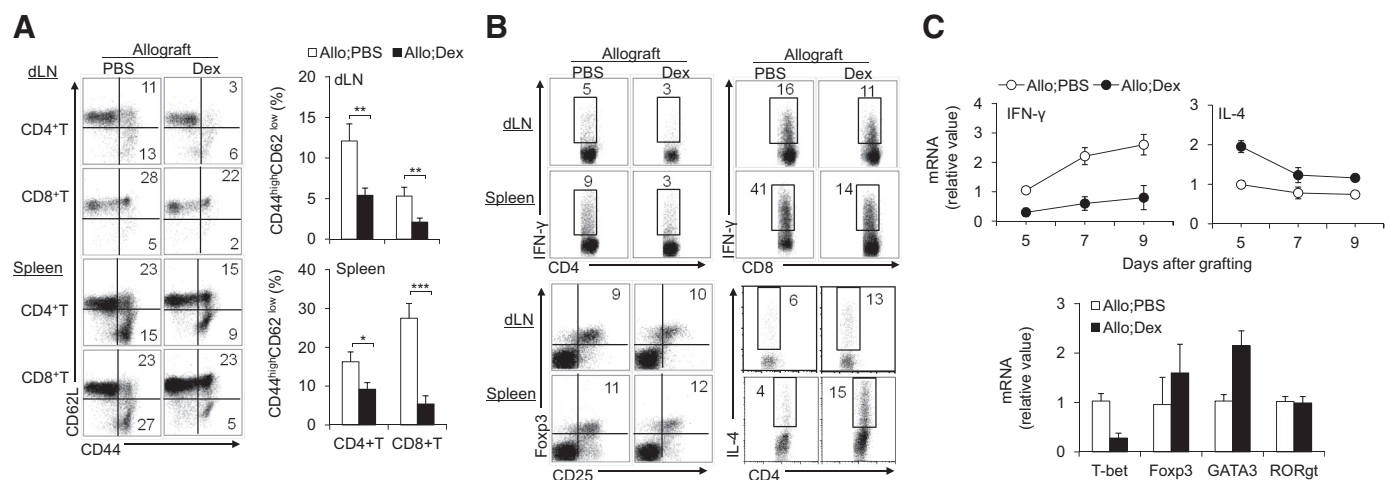
Figure 5. Dex modulates reciprocal Th1 and Th2 cell differentiation in allograft recipients. (A) On Days 8–11, the CD44 and CD62L expression patterns on CD4$^+$ T or CD8$^+$ T cells of the dLNs and spleen in allograft recipients were analyzed with FCM, with a representative FCM figure shown, and the data summarized (right). (B) On Days 8–11, the IFN-γ, IL-4, and Foxp3 expression patterns in the CD4$^+$ T and CD8$^+$ T cells in the dLNs or spleen in the allograft recipient mice were detected with FCM, and representative figures are shown. (C) At the indicated time-points, the mRNA expression of IFN-γ and IL-4 of MDSCs isolated from the graft was determined by real-time PCR and the data summarized. (Right) On Days 9–11, the transcriptional factor mRNA level of T-bet, Foxp3, GATA3, and RORγt in the MDSCs isolated from the graft was determined with real-time PCR, and data were summarized. Data are representative of three to four (A and B) or two (C) independent experiments (n=3–5). *$P <$ 0.05; **$P <$ 0.01; and ***$P <$ 0.001 compared with the indicated groups.

creased and diminished significantly, respectively, in the Dex-treated MDSC cotransferred groups. Furthermore, the transcriptional factor expression T-bet and GATA3, but not Foxp3, were diminished and increased significantly, respectively, in the Dex-treated MDSC transferred groups (Fig. 6E). Altogether, these data suggest that in allograft recipient mice, Dex-induced MDSCs reciprocally regulate the differentiation of Th1 and Th2 and consequently, prolong allograft survival.

Dex-induced MDSCs suppress T cell activation and modulate T cell differentiation via NO production.

NO production has been suggested as a critical component of the immunosuppressive activity of MDSCs [29]. We thus measured the NO levels in the allograft mice. In agreement, the average NO level was substantially higher in the Dex-treated allograft recipient mice than the control (**Fig. 7A**). In addition, the mRNA level of iNOS, a NO-producing metabolic enzyme, was induced significantly, whereas the mRNA level of arginase, a metabolic enzyme sharing the same substrate with iNOS, was reduced in CD11b$^+$Gr1$^+$ MDSCs following Dex treatment in the allograft recipient mice (Fig. 7A). To determine whether NO production is an essential component in MDSC prolongation of allograft survival, we applied L-NMMA, an inhibitor of iNOS, to the functional in vitro assay. L-NMMA reduced NO production significantly (Supplemental Fig. 3) and reduced the immunosuppressive activity efficiently in MDSCs isolated from Dex-treated allograft recipient mice, as indicated by the T cell proliferation assay (Fig. 7B). Whereas cotransfer of MDSCs isolated from Dex-treated allograft recipient mice along with T cells induced a reciprocal differentiation of Th1 and Th2, L-NMMA diminished this effect significantly (Fig. 7C and D). To determine whether arginine depletion caused by increased iNOS contributes to the immunosuppressive effects of the MDSCs induced by Dex, we added L-arginine to the culture system. Arginine addition did not significantly change the suppressive activity of the Dex-induced MDSCs (data not shown), indicating that NO production, but not arginine depletion, contributes to MDSC-mediated immunomodulation in allograft rejection. Furthermore, the in vivo role of iNOS was investigated in an adoptive-transfer model using B6 recipients pretreated with an anti-Gr1 antibody to deplete Gr1$^+$ cells. CD11b$^+$Gr1$^+$ cells were isolated from PBS- or Dex-treated allograft recipient mice, cotreated with PBS or Dex and L-NMMA, and then adoptively transferred into recipients. L-NMMA cotreatment significantly reversed the effect of Dex on allograft survival (Fig. 7E). Taken together, NO is required for Dex-induced MDSC amelioration of allograft immune rejection-associated inflammation.

DISCUSSION

Although emerging evidence indicates that GCs (such as Dex) ameliorate the immune-mediated allograft rejection associated with inflammation, the mechanism remains unclear. Here, we show that MDSCs are essential for Dex to relieve allograft-immune rejection. Further mechanistic insight was obtained by demonstrating the modulatory effects of Dex–GR signaling in MDSCs. By targeting the GR signaling pathway, Dex potentiates MDSC recruitment and function, as well as promoting the reciprocal differentiation of Th2 and Th1 in ameliorating allograft inflammatory injuries. This is consistent with the previously established role of MDSCs in limiting immune rejection inflammatory injury in the course of clinical transplantation [34]. This study reveals a previously unknown feature of
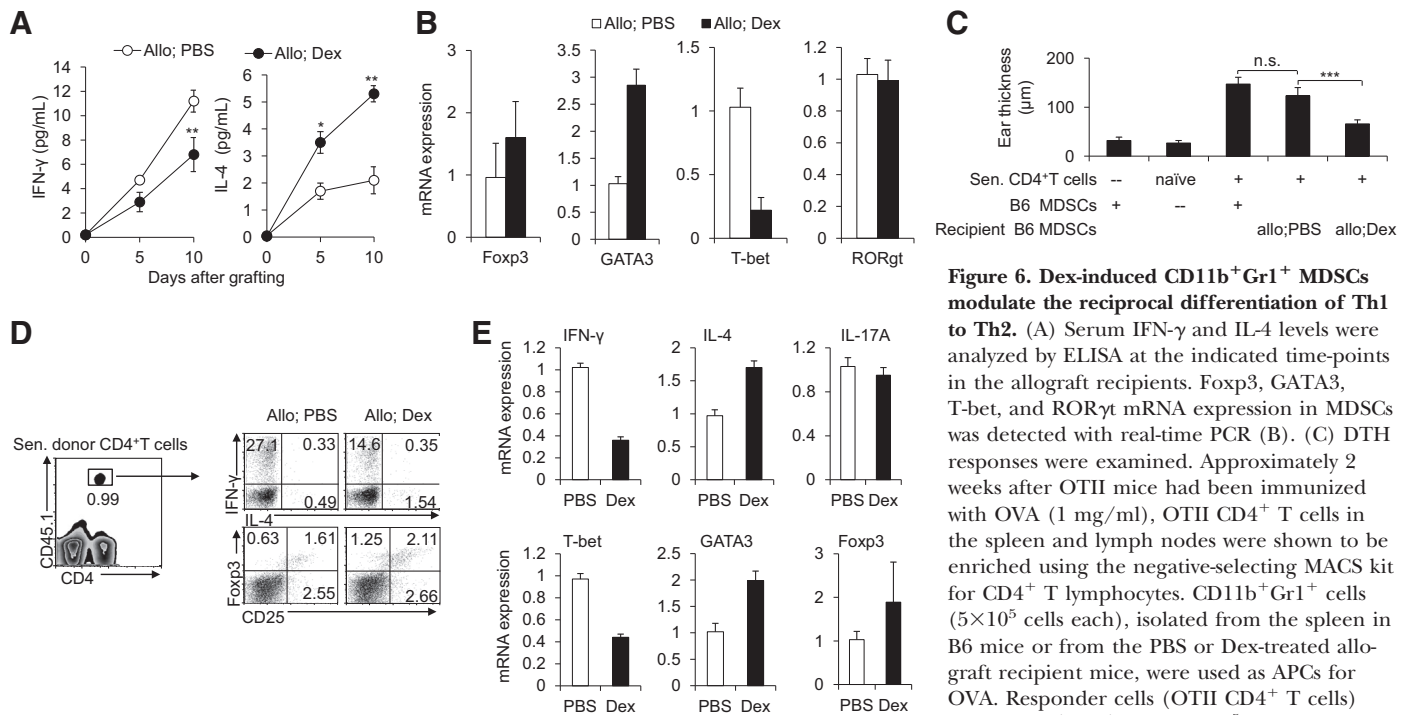
Figure 6. Dex-induced CD11b$^+$Gr1$^+$ MDSCs modulate the reciprocal differentiation of Th1 to Th2. (A) Serum IFN-γ and IL-4 levels were analyzed by ELISA at the indicated time-points in the allograft recipients. Foxp3, GATA3, T-bet, and RORγt mRNA expression in MDSCs was detected with real-time PCR (B). (C) DTH responses were examined. Approximately 2 weeks after OTII mice had been immunized with OVA (1 mg/ml), OTII CD4$^+$ T cells in the spleen and lymph nodes were shown to be enriched using the negative-selecting MACS kit for CD4$^+$ T lymphocytes. CD11b$^+$Gr1$^+$ cells (5×10^5 cells each), isolated from the spleen in B6 mice or from the PBS or Dex-treated allograft recipient mice, were used as APCs for OVA. Responder cells (OTII CD4$^+$ T cells) and CD11b$^+$Gr1$^+$ cells (5×10^5 cells each) with OVA were injected i.d. into the pinnate of naïve CD45.1$^+$ B6 mice. The changes in ear thickness were measured using an Engineer's micrometer, 48 h after the challenge. The ear-thickness changes were calculated by subtracting the thickness of the same ear before injection from that after injection. Sen., sensitized. (D) The dLN lymphocytes were isolated and IFN-γ, IL-4, and Foxp3 expression in the donor CD4$^+$ T cells analyzed with intracellular staining, and a representative figure is shown. The mRNA of IFN-γ, IL-4, IL-17A, T-bet, GATA3, and Foxp3 was analyzed with real-time PCR (E). Data are representative of three (A and B) or two (C–E) independent experiments (*n*=3–6). *$P < 0.05$; **$P < 0.01$; and ***$P < 0.001$ compared with the indicated groups.

MDSC function in immunohomeostasis, i.e., the reprogramming of T cell differentiation from Th1 to Th2, which represents a novel mechanism of GC-ameliorated transplant immunological rejection by a targeting of the GC–GR signaling pathway.

GCs, which have been widely used in treating inflammatory disorders, including amelioration of the transplant-rejection response, are well-known for their regulation of the immune system. A recent study showed that MDSCs accumulated in prednisone-treated human kidney transplant recipients and mediated CD4$^+$Foxp3$^+$ T$_{reg}$ expansion [15]. However, the anti-inflammatory effect and important role in transplant immunology of GCs are highly complex. In the present study, typical immunological murine allograft models were used to investigate the effect of GCs and role of the GR signaling pathway in modulating transplant rejection. We showed that Dex, via its targeting of the GR signaling pathway, directly modulated MDSC NO production and consequently, directed the reciprocal differentiation of T cells in the allograft immune-inflammatory injury.

There are various molecular mechanisms involved in GC resistance or hypersensitivity and GR expression seems to be a key one [35, 36]. These mechanisms are important for the regulation of cell and tissue-specific GC sensitivity and are pathologically modified in certain clinical conditions such as AIDS, GC-resistant asthma, rheumatoid arthritis and familial GC resistance, among others [36]. GR signaling has been

shown to have an important role in promoting the expansion of MDSCs in a murine model of trauma [37]. Moreover, MDSCs have been shown to accumulate in traumatized hosts and can be induced in in vitro models [38–40]. In addition, in vivo studies have demonstrated the promotive effect of GCs on MDSCs in endotoxin immunosuppressed mice [41], and that MDSCs accumulate and contribute to kidney and cardiovascular transplantation tolerance [13, 14]. In the present study, we demonstrate the intrinsic regulatory effects of MDSCs in prolonging allograft survival and show a previously unknown feature of MDSC function in immunohomeostasis, i.e. the reprogramming of T cell differentiation from Th1 to Th2, which represents a novel mechanism of GC amelioration of transplant immunological rejection by targeting the GR signaling pathway.

MDSC chemoattractant factors, including CXC chemokines and inflammatory mediators, released by resident cells or other immune cells [29–32], recruit MDSCs to inflammatory sites during the inflammatory response. In this acute skin transplantation model, Dex-treated mice expressed a higher level of CXCL1 and CXCL2, as well as CXCR2 (the receptor CXCL1 and CXCL2). Importantly, blockade of CXCR2 with a CXCR2 mAb or blocking GR with RU486 significantly reverses the graft survival and MDSC recruitment in Dex-treated mice. It is thought that MDSC recruitment is critically required for Dex to prolong allograft survival. The increase in Dex-induced MDSC recruitment significantly ameliorated graft rejection
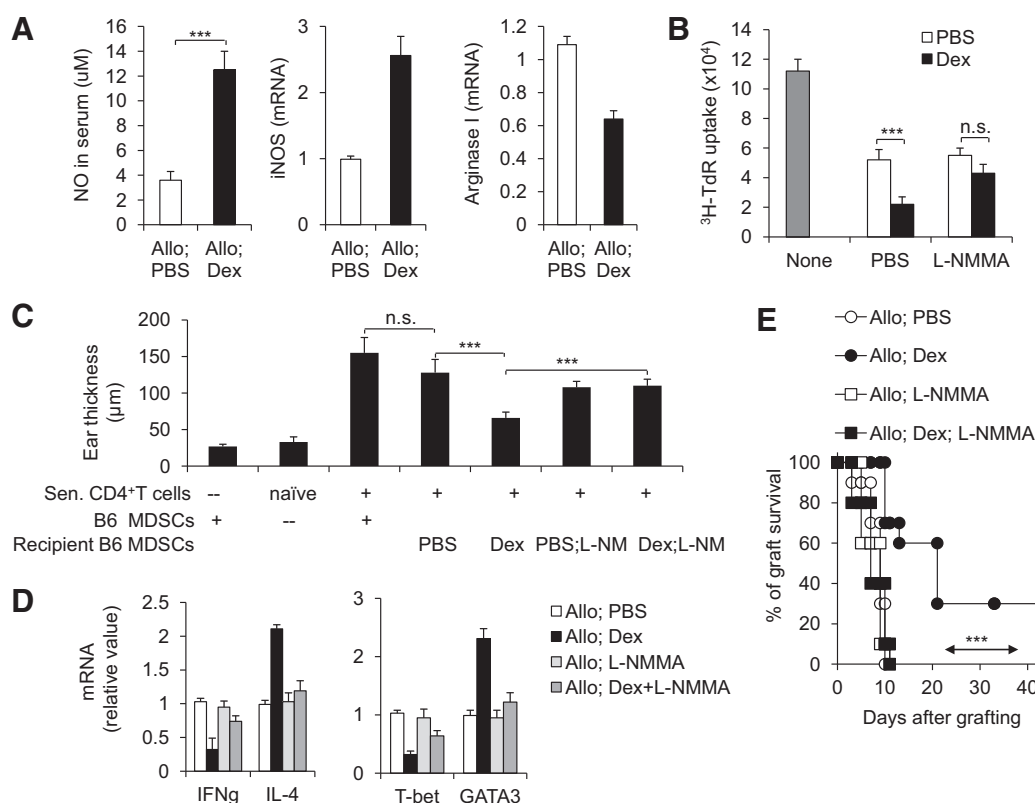
Figure 7. Dex-induced CD11b^{+}Gr1^{+} MDSCs promote reciprocal differentiation of Th1 to Th2 through NO production. (A) Significantly higher NO levels in serum and higher iNOS mRNA and lower Arg1 mRNA in splenic CD11b^{+}Gr1^{+} cells from Dex-treated allograft mice compared with PBS-treated control mice. Blocking NO production significantly decreased the inhibitory capacity of Dex-treated CD11b^{+}Gr1^{+} MDSCs in vitro (B) and in vivo DTH (C). (D) In DTH, dLN CD4^{+} T cells were isolated and the mRNA of IFN-γ, IL-4, T-bet, and Foxp3 detected by real-time PCR. (E) The indicated allograft recipient mice, which were treated or not with L-NMMA (80 mg/kg, gavage daily). Mice were killed 8 days later, and 1×10^6 CD11b^{+}Gr1^{+} cells were sorted from the spleen and transferred into the same B6 recipient mice pretreated with an anti-Gr1 mAb (0.5 mg), 1 day earlier. Allograft recipient mice underwent skin transplantation, 12 h after cell transfer, and the graft-survival curve was plotted (n=10). Data are representative of three (A and B) or two (C and D) independent experiments (n=3–5). ***$P <$ 0.001 compared with the indicated groups.

and enhanced inhibitory activity (Fig. 3A and B), while decreasing proinflammatory cytokine production (Fig. 3C). Whereas these data suggest that the accumulation and recruitment of Dex-induced MDSCs play a critical role, from the present results, it is still not possible to discriminate the effects of MDSC recruitment from decreased inhibition of T cell function in vivo in the context of Dex prolongation of allograft survival.

As is well-known, GC–GR reciprocally reprograms the differentiation of Th1 and Th2 [7]. Notably, GCs (such as Dex), one of the important immunosuppressants for transplant-immune rejection injury, target the GR. Our studies suggest that MDSCs contribute to the immunomodulatory functions of GCs. The GC–GR–NO pathway in MDSCs is promising for the development of new therapeutics for transplantation, autoimmunity, cancer, and infection.

AUTHORSHIP

J.L. designed and conducted the mouse allograft skin transplantation and analyzed data. XiaoW. designed and conducted the experiments with cells and mice and analyzed data. Y.B. designed and conducted the experiments with cells and mice, analyzed data, and contributed to the writing of the manuscript. B.S. and H.Y. conducted the experiments with cells. K.S. and Y.C. contributed to writing the manuscript. Y.L., Z.Z., X.C., H.L., and J.W. participated in discussions. L.X. and Xianghui W. designed the experiments, analyzed data, and contributed to the writing of the manuscript. G.L. developed the concept, designed and conducted the experiments with cells and mice, analyzed data, wrote the manuscript, and provided overall direction.

ACKNOWLEDGMENTS

DISCLOSURES

REFERENCES

1. Abraham, S. M., Lawrence, T., Kleiman, A., Warden, P., Medghalchi, M., Tuckermann, J., Saklatvala, J., Clark, A. R. (2006) Antiinflammatory effects of dexamethasone are partly dependent on induction of dual specificity phosphatase 1. *J. Exp. Med.* **203**, 1883–1889.

2. Bhattacharyya, S., Brown, D. E., Brewer, J. A., Vogt, S. K., Muglia, L. J. (2007) Macrophage glucocorticoid receptors regulate Toll-like receptor 4-mediated inflammatory responses by selective inhibition of p38 MAP kinase. *Blood* **109**, 4313–4319.

3. Hackstein, H., Thomson, A. W. (2004) Dendritic cells: emerging pharmacological targets of immunosuppressive drugs. *Nat. Rev. Immunol.* **4**, 24–34.

4. Zheng. G., Zhong, S., Geng, Y., Munirathinam, G., Cha, I., Reardon, C., Getz, G. S., Van, Rooijen, N., Kang, Y., Wang, B., Chen, A. (2013) Dexamethasone promotes tolerance in vivo by enriching CD11clo CD40lo tolerogenic macrophages. *Eur. J. Immunol.* **43**, 219–227.

5. Kang, Y., Xu, L., Wang, B., Chen, A., Zheng, G. (2008) Cutting edge: immunosuppressant as adjuvant for tolerogenic immunization. *J. Immunol.* **180**, 5172–5176.

6. Almawi, W. Y., Hess, D. A., Rieder, M. J. (1998) Multiplicity of glucocorticoid action in inhibiting allograft rejection. *Cell Transplant.* **7**, 511–523.

7. Almawi, W. Y., Melemedjian, O. K., Rieder, M. J. (1999) An alternate mechanism of glucocorticoid anti-proliferative effect: promotion of a Th2 cytokine-secreting profile. *Clin. Transplant.* **13**, 365–374.

8. Ray, P., Arora, M., Poe, S. L., Ray, A. (2012) Lung myeloid-derived suppressor cells and regulation of inflammation. *Immunol. Res.* **50**, 153–158.

9. Liu, G., Bi, Y., Shen, B., Yang, H., Zhang, Y., Wang, X., Liu, H., Lu, Y., Liao, J., Chen, X., Chu, Y. (2014) SIRT1 limits the function and fate of myeloid-derived suppressor cells in tumors by orchestrating HIF-1α-dependent glycolysis. *Cancer Res.* **74**, 727–737.

10. Ostrand-Rosenberg, S., Sinha, P. (2009) Myeloid-derived suppressor cells: linking inflammation and cancer. *J. Immunol.* **182**, 4499–4506.

11. Jayaraman, P., Parikh, F., Lopez-Rivera, E., Hailemichael, Y., Clark, A., Ma, G., Cannan, D., Ramacher, M., Kato, M., Overwijk, W. W., Chen, S. H., Umansky, V. V., Sikora, A. G. (2010) Tumor-expressed inducible nitric oxide synthase controls induction of functional myeloid-derived suppressor cells through modulation of vascular endothelial growth factor release. *J. Immunol.* **188**, 5365–5376.

12. Van, Rompaey, N., Le Moine, A. (2010) Myeloid-derived suppressor cells: characterization and expansion in models of endotoxemia and transplantation. *Methods Mol. Biol.* **677**, 169–180.

13. Dugast, A. S., Haudebourg, T., Coulon, F., Heslan, M., Haspot, F., Poirier, N., Vuillefroy, D. E., Silly, R., Usal, C., Smit, H., Martinet, B., Thebault, P., Renaudin, K., Vanhove, B. (2008) Myeloid-derived suppressor cells accumulate in kidney allograft tolerance and specifically suppress effector T cell expansion. *J. Immunol.* **180**, 7898–7906.

14. Garcia, M. R., Ledgerwood, L., Yang, Y., Xu, J., Lal, G., Burrell, B., Ma, G., Hashimoto, D., Li, Y., Boros, P., Grisotto, M., Van Rooijen, N., Matesanz, R., Tacke, F., Ginhoux, F., Ding, Y., Chen, S. H., Randolph, G., Merad, M., Bromberg, J. S., Ochando, J. C. (2010) Monocytic suppressive cells mediate cardiovascular transplantation tolerance in mice. *J. Clin. Invest.* **120**, 2486–2496.

15. Luan, Y., Mosheir, E., Menon, M. C., Wilson, D., Woytovich, C., Ochando, J., Murphy, B. (2013) Monocytic myeloid-derived suppressor cells accumulate in renal transplant patients and mediate CD4(+) Foxp3(+) Treg expansion. *Am. J. Transplant.* **13**, 3123–3131.

16. Rosenberg, A. S., Mizuochi, T., Singer, A. (1988) Evidence for involvement of dual-function T cells in rejection of MHC class I disparate skin grafts. Assessment of MHC class I alloantigens as in vivo helper determinants. *J. Exp. Med.* **168**, 33–45.

17. Rosenberg, A. S., Munitz, T. I., Maniero, T. G., Singer, A. (1991) Cellular basis of skin allograft rejection across a class I major histocompatibility barrier in mice depleted of CD8+ T cells in vivo. *J. Exp. Med.* **173**, 1463–1471.

18. Mayumi, H., Nomoto, K., Good, R. A. (1988) A surgical technique for experimental free skin grafting in mice. *Jpn. J. Surg.* **18**, 548–557.

19. Corry, R. J., Winn, H. J., Russell, P. S. (1973) Primarily vascularized allografts of hearts in mice. The role of H-2D, H-2K, and non-H-2 antigens in rejection. *Transplantation* **16**, 343–350.

20. Siemionow, M., Demir, Y., Mukherjee, A., Klimczak, A. (2005) Development and maintenance of donor-specific chimerism in semi-allogenic and fully major histocompatibility complex mismatched facial allograft transplants. *Transplantation* **79**, 558–567.

21. Sun, B., Hu, X., Liu, G., Ma, B., Xu, Y., Yang, T., Shi, J., Yang, F., Li, H., Zhang, L., Zhao, Y. (2014) Phosphatase Wip1 negatively regulates neutrophil migration and inflammation. *J. Immunol.* **192**, 1184–1195.

22. Schumann, J., Prockl, J., Kiemer, A. K., Vollmar, A. M., Bang, R., Tiegs, G. (2003) Silibinin protects mice from T cell-dependent liver injury. *J. Hepatol.* **39**, 333–340.

23. Cripps, J. G., Wang, J., Maria, A., Blumenthal, I., Gorham, J. D. (2010) Type 1 T helper cells induce the accumulation of myeloid-derived suppressor cells in the inflamed Tgfb1 knockout mouse liver. *Hepatology* **52**, 1350–1359.

24. Liu, G., Burns, S., Huang, G., Boyd, K., Proia, R.l., Flavell, R.A., Chi, H. (2009) The receptor S1P1 overrides regulatory T cell-mediated immune suppression through Akt-mTOR. *Nat. Immunol.* **10**, 769–777.

25. Liu, G., Bi, Y., Wang, R., Yang, H., Zhang, Y., Wang, X., Liu, H., Lu, Y., Zhang, Z., Chen, W., Chu, Y., Yang, R. (2014) Targeting S1P1 receptor protects against murine immunological hepatic injury through myeloid-derived suppressor cells. *J. Immunol.* **192**, 3068–3079.

26. Liu, G., Ma, H., Qiu, L., Li, L., Cao, Y., Ma, J., Zhao, Y. (2011) Phenotypic and functional switch of macrophages induced by regulatory CD4+CD25+ T cells in mice. *Immunol. Cell Biol.* **89**, 130–142.

27. Liu, G., Hu, X., Sun, B., Yang, T., Shi, J., Zhang, L., Zhao, Y. (2013) Phosphatase Wip1 negatively regulates neutrophil development through p38 MAPK-STAT1. *Blood* **121**, 519–529.

28. Liu, G., Bi, Y., Wang, R., Shen, B., Zhang, Y., Yang, H., Wang, X., Liu, H., Lu, Y., Han, F. (2013) Kinase AKT1 negatively controls neutrophil recruitment and function in mice. *J. Immunol.* **191**, 2680–2690.

29. Sander, L. E., Sackett, S. D., Dierssen, U., Beraza, N., Linke, R. P., Muller, M., Blander, J. M., Tacke, F., Trautwein, C. (2010) Hepatic acute-phase proteins control innate immune responses during infection by promoting myeloid-derived suppressor cell function. *J. Exp. Med.* **207**, 1453–1464.

30. Chen, H. W., Chen, H. Y., Wang, L. T., Wang, F. H., Fang, L.W., Lai, H. Y., Chen, H. H., Lu, J., Hung, M. S., Cheng, Y., Chen, M. Y., Liu, S. J., Chong, P., Lee, O. K., Hsu, S. C. (2013) Mesenchymal stem cells tune the development of monocyte-derived dendritic cells toward a myeloid-derived suppressive phenotype through growth-regulated oncogene chemokines. *J. Immunol.* **190**, 5065–5077.

31. Schlecker, E., Stojanovic, A., Eisen, C., Quack, C., Falk, C. S., Umansky, V., Cerwenka, A. (2012) Tumor-infiltrating monocytic myeloid-derived suppressor cells mediate CCR5-dependent recruitment of regulatory T cells favoring tumor growth. *J. Immunol.* **189**, 5602–5011.

32. Dilek, N., Poirier, N., Usal, C., Martinet, B., Blancho, G., Vanhove, B. (2012) Control of transplant tolerance and intragraft regulatory T cell localization by myeloid-derived suppressor cells and CCL5. *J. Immunol.* **188**, 4209–4216.

33. Kodumudi, K. N., Weber, A., Sarnaik, A. A., Pilon-Thomas, S. (2011) Blockade of myeloid-derived suppressor cells after induction of lymphopenia improves adoptive T cell therapy in a murine model of melanoma. *J. Immunol.* **189**, 5147–5154.

34. Chen, S., Akbar, S. M., Abe, M., Hiasa, Y., Onji, M. (2011) Immunosuppressive functions of hepatic myeloid-derived suppressor cells of normal mice and in a murine model of chronic hepatitis B virus. *Clin. Exp. Immunol.* **166**, 134–142.

35. Mirani, M., Elenkov, I., Volpi, S., Hiroi, N., Chrousos, G. P., Kino, T. (2012) HIV-1 protein Vpr suppresses IL-12 production from human monocytes by enhancing glucocorticoid action: potential implications of Vpr coactivator activity for the innate and cellular immunity deficits observed in HIV-1 infection. *J. Immunol.* **169**, 6361–6368.

36. Kino, T., Chrousos, G. P. (2001) Glucocorticoid and mineralocorticoid resistance/hypersensitivity syndromes. *J. Endocrinol.* **169**, 437–445.

37. Zhang, K., Bai, X., Li, R., Xiao, Z., Chen, J., Yang, F., Li, Z. (2012) Endogenous glucocorticoids promote the expansion of myeloid-derived suppressor cells in a murine model of trauma. *Int. J. Mol. Med.* **30**, 277–282.

38. Barczyk, K., Ehrchen, J., Tenbrock, K., Ahlmann, M., Kneidl, J., Viemann, D., Roth, J. (2010) Glucocorticoids promote survival of anti-inflammatory macrophages via stimulation of adenosine receptor A3. *Blood* **116**, 446–455.

39. Ehrchen, J., Steinmuller, L., Barczyk, K., Tenbrock, K., Nacken, W., Eisenacher, M., Nordhues, U., Sorg, C., Sunderkotter, C., Roth, J. (2007) Glucocorticoids induce differentiation of a specifically activated, anti-inflammatory subtype of human monocytes. *Blood* **109**, 1265–1274.

40. Varga, G., Ehrchen, J., Tsianakas, A., Tenbrock, K., Rattenholl, A., Seeliger, S., Mack, M., Roth, J., Sunderkoetter, C. (2008) Glucocorticoids induce an activated, anti-inflammatory monocyte subset in mice that resembles myeloid-derived suppressor cells. *J. Leukoc. Biol.* **84**, 644–650.

41. Rearte, B., Maglioco, A., Balboa, L., Bruzzo, J., Landoni, V. I., Laborde, E. A., Chiarella, P., Ruggiero, R. A., Fernandez, G. C., Isturiz, M. A. (2010) Mifepristone (RU486) restores humoral and T cell-mediated immune response in endotoxin immunosuppressed mice. *Clin. Exp. Immunol.* **162**, 568–577.